



ARTICLE

## Structure and Properties of PLA Composite Enhanced with Biomass Fillers from Herbaceous Plants

Haining Na<sup>1,\*</sup>, Juncheng Huang<sup>1</sup>, Hongguang Xu<sup>2</sup>, Fei Liu<sup>3</sup>, Liangke Xie<sup>1</sup>, Baoqing Zhu<sup>3</sup>, Jiuchen Wang<sup>2</sup> and Jin Zhu<sup>1,\*</sup>

<sup>1</sup>Key Laboratory of Bio-Based Polymeric Materials of Zhejiang Province, Ningbo Institute of Materials Technology and Engineering, Chinese Academy of Sciences, Ningbo, 315201, China

<sup>2</sup>Weifang Yunding New Material Technology Company Limited, Weifang, 262100, China

<sup>3</sup>Jilin Hwood Technology Company Limited, Dunhua, 133712, China

\*Corresponding Authors: Haining Na. Email: nahaining@nimte.ac.cn; Jin Zhu. Email: jzhu@nimte.ac.cn

Received: 26 May 2022 Accepted: 01 August 2022

### ABSTRACT

PLA composites containing biomass fillers from the three herbaceous plants such as reed, wheat stalk, and coconut fiber with length and diameter at the scale of several millimeters were prepared without using additives. The reinforcement effect on the properties of PLA/biomass filler composites is investigated. The research results show that the PLA/biomass filler composites exhibit good stiffness, flexural strength, and impact toughness. Among the three kinds of biomass fillers, reed reinforced PLA composites show optimal mechanical properties. When filled with 40%–50% reed, the flexural moduli of the composites are over 7000 MPa. Flexural strength retains at the same level of pure PLA. The notch impact strength reaches to  $4.50 \pm 0.73$  kJ/m<sup>2</sup>, which is 2.06 times higher than that of pure PLA. Furthermore, the introduction of biomass fillers increases the crystallization ability of PLA and does not increase the water absorption of the composites. This research demonstrated that PLA composites prepared with biomass fillers from the herbaceous plants (namely herb plastic composites, HPCs) is a material with good comprehensive mechanical properties while retaining the intrinsic particularity of biological sources.

### KEYWORDS

PLA; biomass filler; herb plastic composites

## 1 Introduction

In recent years, carbon neutrality and environmental sustainability has become an important driver of development in all sectors. As an important renewable organic carbon resource with tremendous reserves in nature [1,2], the conversion and utilization of biomass has attracted extensive attention to replace fossil resources. Since biomass is produced by the absorption of carbon dioxide through the photosynthesis of plants, the conversion of biomass into bio-based materials is undoubtedly a necessary step to realize carbon sequestration and carbon reduction. It plays an important role in promoting carbon neutral cycle on the ground to support sustainable development [3–6].

Biomass is widely used as a filler in the design and manufacture of polymer composites [7]. A good example is wood plastic composites (WPCs). They are composite materials mainly constructed from



plastic, wood flour and some additives (including compatibilizer, toughening agent and inorganic fillers). Wood flour is mainly generated from the wood waste of manmade board in the industrial field [8]. The types of wood generally mention poplar, masson pine and so on. The size of wood flour for WPCs is usually controlled at 40–200 mesh. Besides improving the utilization rate and processability of wood waste, WPC could show the appearance and the good characteristics to mimic wood materials, including the strength and toughness. WPC has achieved great success in the wood-like materials and synthetic board industry [8–10]. With current technology, WPCs are increasingly produced from waste materials and residual products from the wood and agricultural industry rather than raw wood flour, such as sawdust, rice straw flour, and pulping sludge (namely lignified powders and fibers) [7]. WPCs have been widely applied in decking, railing, siding, fences, windows, door frames, and playground equipment [11,12].

In order to create polymer composites with better environmental sustainability, biodegradable polymers are gradually gaining popularity for application in WPCs, due to their sustainability both in sourcing raw material and biodegradation [13]. Among the natural and synthetic biodegradable polymers, poly (lactic acid) (PLA) has the greatest commercial application [14,15]. On a similar basis to WPC, many powdered biomass fillers (including wood flour, cellulose, lignin flour, starch, and etc.) [16] are used to blend into PLA with the aim of overcoming one of the primary drawbacks of PLA [17,18], the price to performance ratio, in order to optimize its use in specific commercial applications. The processing of PLA with powdered biomass fillers can be easily achieved by traditional extrusion. Although the stiffness, hardness and flexural modulus of the PLA composites with the introduction of powdered biomass fillers can be improved, it inevitably leads to the decrease of tensile strength, bending strength and toughness. As a result, the comprehensive mechanical properties of the PLA/biomass filler composites are significant decrease. In practical applications, a large number of additives and inorganic powders (for example, calcium carbonate, talc, mica, and etc.) usually have to be used to adjust the properties of the composites [12]. However, the use of inorganic powders in PLA not only reduces the intrinsic particularity of biological sources of the PLA/biomass filler composites to some extent, but also induces the unexpected decrease in comprehensive properties of the obtained PLA based composites to use as biodegradable polymer products.

In fact, the natural biomass, no matter comes from woody or herbaceous plants, due to the growth mode of plants, is essentially rich with plant fibers. Generally, polymer composites prepared with fibrous fillers exhibit excellent comprehensive mechanical properties [19]. Therefore, if the biomass filler can remain at a larger size in the PLA/biomass filler composites, it will better maintain the structure of inherent plant fibers in biomass filler. The performances of the PLA composites are expected to improve. In our previous work [20], large sized jute fiber (at the scale of several millimeters to one centimeter) was blended into PLA for the preparation of biodegradable polymer composites with high performances. In addition, Fujiura et al. [21] and Liu et al. [22] respectively have used particular extrusion and injection molding to prepare PLA based composites with large sized jute yarn. An improvement in the comprehensive properties of PLA based composites by jute fiber was noted [21,22].

In this study, biomass fillers at the scale of several millimeters derived mainly from three types of herbaceous plants including reed, stalk, and coconut fiber are used to prepare particular PLA/biomass filler composites. Because the biomass filler is mainly from herbaceous plant, the composites should be known as herb polymer composites (HPCs). During our research, PLA is used to prepare HPCs without other additives as a model. The effect of the biomass fillers on the properties of the PLA/biomass filler composites was investigated. Furthermore, microstructure, morphology, mechanical and thermal properties, and water resistance of PLA/biomass filler composites with different amount of biomass filler is explored.

## 2 Experimental Sections

### 2.1 Materials

PLA (REVOKE 190) was bought from Zhejiang Hisun Biomaterials Co., Ltd. (China). Reed (Rd) and wheat stalk (WS) were collected from Dongying and Gaomi (Shandong, China) by Weifang Yunding New Material Technology Co., Ltd. (China), respectively. Coconut fiber (CF, from Vietnam) was purchased from Hainan Yeyi Trading Co., Ltd. (China). All the biomass fillers were dried until the moisture content was less than 3%. After that, the biomass fillers were shortly-chopped and then directly used to prepare PLA/biomass filler composites without further purification. After shortly-chopped, the length of reed, wheat stalk and coconut fiber are all around 1–2 cm. And the diameters of reed, wheat stalk and coconut fiber are 0.134, 0.129 and 0.438 mm in average, respectively.

### 2.2 Preparation of PLA/Biomass Filler Composites

Before processing, PLA was dried in a drying oven for 4 h at 100°C. After that, PLA and biomass fillers were processed with a high-speed blending machine (YK-10L, produced by Weifang Yunding New Material Tech. Co., Ltd. in China) with the mass ratio at 70/30, 60/40, 50/50, and 40/60. Mixing speed and initial working current were respectively set at 2800 rpm and 100 A, respectively. During blending, until the working current reaches 125 A, the blending of PLA and biomass fillers automatically stopped and then unloaded. The process of processing lasted ~45 s.

An extruder (SJ100-13-1, from Nanjing Jiyea Extrusion Equipment Co., Ltd., China) was used to further treat the obtained PLA/biomass filler mixtures at 180°C. PLA/biomass filler composites were formed and then cut into pellets (with the length at ~0.8 mm and the thickness at ~0.5 mm). An injection molding machine (DYW800, from Ningbo Deya Plastic Machinery Co., Ltd., China) was used to mold pure PLA and the PLA/biomass filler composites into standard samples for further test (following the national standard, Plastics-Determination of flexural properties (GB/T 9341-2008) and the international standard, Plastics-Determination of charpy, Impact strength, ISO179-1.98)). During injection molding, the temperature was set at 170°C–190°C.

### 2.3 Characterizations

A testing machine (CMT 4304, from Sansi Taijie, Zhuhai, China) was used to test the flexural properties of the obtained the samples of PLA/biomass filler composites (length ~80 mm, width 10 mm and thickness ~4 mm). According to Chinese standard (GB/T 9341-2008), the span was set at 64 mm, and the crosshead speed was 10 mm/min constantly. Impact tester with 22 J pendulum (KBC-750-8, from Sansi Taijie, Zhuhai, China) was utilized to measure the notched impact (length ~80 mm, width 10 mm, thickness ~4 mm and Type C notch) of the samples of PLA/biomass filler composites according to the international standard (ISO179-1.98). Average results of all the mechanical properties were calculated from three repeated tests. A hardness tester (LX-D, from Handpi, Germany) was used to examine the Shore hardness of the samples (thickness ~4 mm) of PLA/biomass filler composites.

5~10 mg sample of each PLA/biomass filler sample was used for the differential scanning calorimetry (DSC) analysis. The DSC test was run on a Mettler-Toledo TGA/DSC1 tester under a high-purity nitrogen atmosphere. The temperature was controlled from 25°C to 200°C with the heating rate of 10 °C/min. Melting enthalpy and crystallinity ( $Cr$ ) of pure PLA and PLA/biomass filler composites was calculated from the DSC curves. Thermogravimetric analysis (TGA) was carried out on the same TGA/DSC1 tester. Each sample with the mass at 5–10 mg was used to record the TGA curve under dry nitrogen atmosphere. The temperature range was set from 50°C to 800°C with the heating rate at 20 °C/min. Thermal properties of the PLA/biomass filler composites such as the temperature at 5% weight loss ( $T_{5\%}$ ), residual mass at 800°C ( $M_{800}$ ), crystallization temperature and melting temperature were respectively recorded in Table 1, respectively. Fourier transform infrared (FT-IR) spectra of the PLA/biomass filler composites were

characterized by a spectrophotometer (Cary660+620, from Agilent, USA) with the wave number range of 4000–400  $\text{cm}^{-1}$ , and the scanning frequency was set at 32 times. The selected area rich with biomass fillers in composites was examined by FT-IR test.

**Table 1:** Thermal properties of PLA/biomass filler composites with reed, wheat stalk, and coconut fiber

Samples	$T_{5\%}$ (°C)	$M_{800}$ (%)	$T_{cc}$ (°C)	$T_m$ (°C)	$\Delta H_{cc}$ (J/g)	$\Delta H_c$ (J/g)	$Cr^*$ (%)
Pure PLA	342.0	0	96.1	174.7	22.73	51.6	31.0
Rd 30	289.4	5.5	91.0	174.6	16.60	36.73	30.9
Rd 60	274.5	13.2	89.7	173.7	7.02	23.78	45.1
WS 30	273.7	8.0	85.9	171.0 175.3	13.89	34.05	31.0
WS 60	263.6	17.4	85.8	167.9 173.7	6.16	24.33	48.8
CF 30	267.7	6.9	94.5	176.5	11.43	32.28	32.0
CF 60	229.9	15.3	86.9	172.8	6.71	23.31	44.6

Note:  $Cr^*$  is calculated with respect to the melt enthalpy of 100% crystalline PLA ( $\Delta H_c^0$ , 93 J/g).  $Cr = (\Delta H_c - \Delta H_{cc}) / (f \Delta H_c^0)$ .  $\Delta H_c$ ,  $\Delta H_{cc}$  and  $f$  denote enthalpies of crystallization, enthalpies of cold crystallization and practical amount of PLA in composites, respectively.

The structure and morphology of biomass fillers (Rd, WS, and CF) in the PLA/biomass filler composites were observed by a scanning electron microscope (SEM, EV018, Zeiss, Germany). The test samples were prepared by cryogenic fracture under liquid nitrogen and then observed by SEM after sputter coated with platinum. The biomass fillers in the PLA/biomass filler composites were also taken out by dissolving PLA with chloroform. After drying, the biomass fillers were observed by optical microscope (BX51, Olympus, Japan). Distributions of length and diameter of the biomass fillers were also calculated to show the structure and morphology.

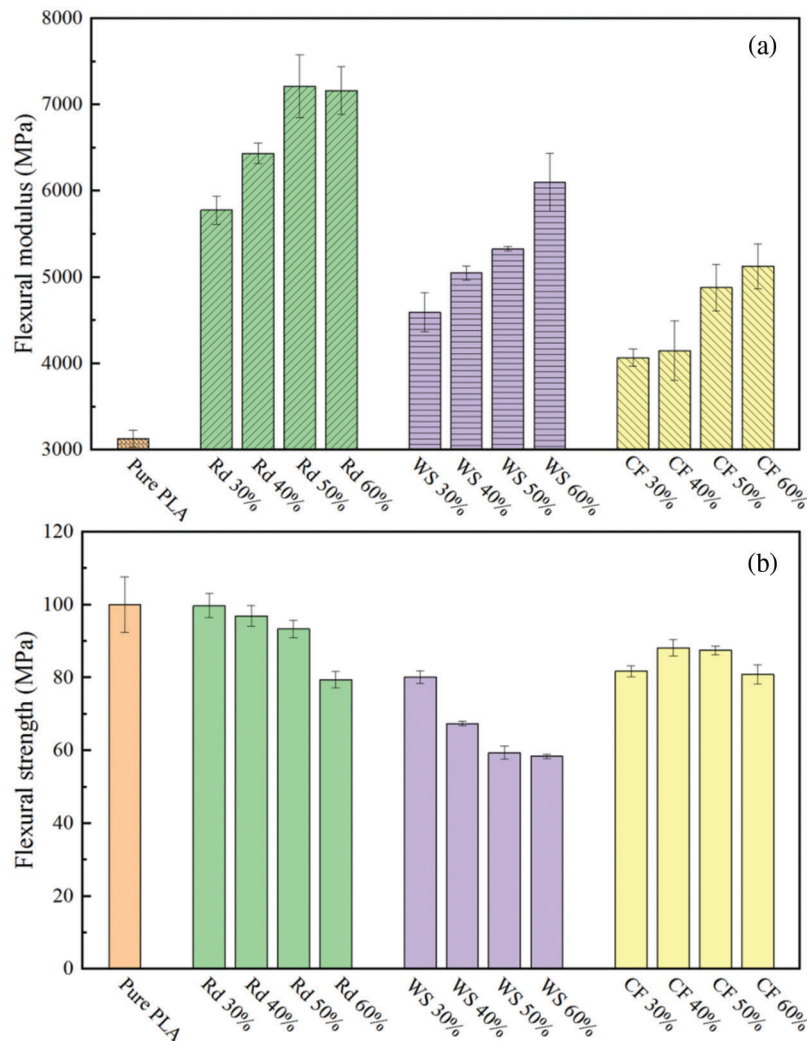
Bruker D8 Advance X-ray Diffractometer (made in Germany) was used for the X-ray diffraction (XRD) analysis of the PLA/biomass filler composites. The intensity of XRD diffraction was measured with  $\text{Cu K}\alpha$  radiation. The  $2\theta$  range was controlled between  $5^\circ$  and  $65^\circ$ .

Test of water absorption was carried out by soaking the sample of PLA/biomass filler composites in water for 48 h at room temperature. The change of mass and size of the samples of PLA/biomass filler composites are tested.

### 3 Results and Discussion

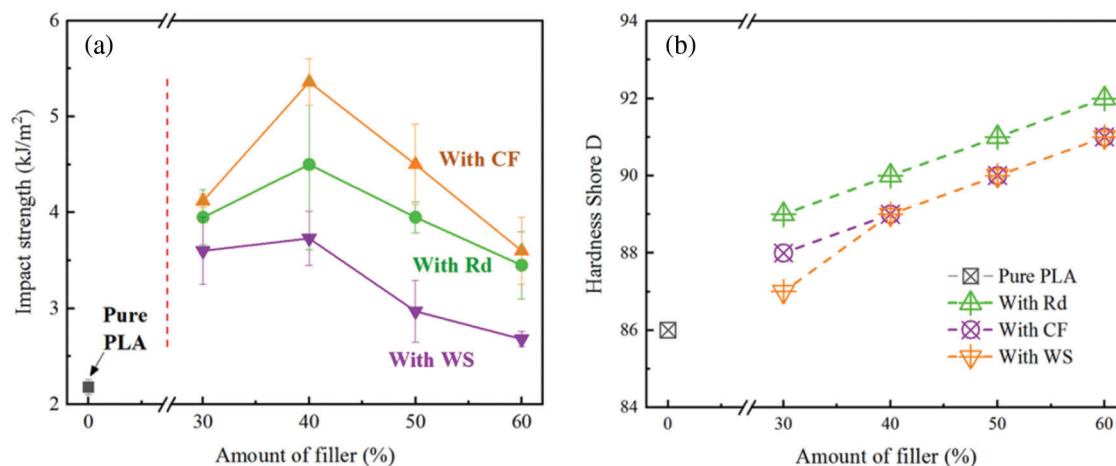
#### 3.1 Mechanical Properties

Fig. 1 illustrates the flexural moduli and strengths of the PLA/biomass filler composites with Rd, WS, and CF. By adding biomass fillers from herbaceous plant, the flexural moduli of the PLA/biomass filler composites sharply increased over 5000 MPa. The more content of the biomass filler was included, the higher the flexural modulus would be. With the addition of 50%–60% Rd, the flexural moduli of the composites reached to the highest value at  $\sim 7000$  MPa (Fig. 1a), which was higher than the composites with WS and CF. As for flexural strengths, the situation was different. From Fig. 1b, at 30%–50% Rd, the flexural strengths of the PLA/biomass filler composites basically remained at the level of pure PLA. However, when using WS and CF in the PLA/biomass filler composites, the flexural strengths decreased by 20%–40%. It indicated the addition of biomass fillers in PLA caused a certain degree of decline in flexural strengths.



**Figure 1:** Flexural modulus (a) and flexural strength (b) of PLA/biomass filler composites with reed, wheat stalk and coconut fiber at different filling amount

Fig. 2a shows the impact strengths of pure PLA and the PLA/biomass filler composites. Pure PLA only showed the impact strength at  $2.18 \pm 0.08 \text{ kJ/m}^2$ . By using biomass filler, the notch impact strengths of the PLA/biomass filler composites were obviously improved. With 30%–60% WS, the notch impact strengths were increased to  $2.68$ – $3.73 \text{ kJ/m}^2$ , which were higher than that of pure PLA. With 40% WS, the value of notch impact strength reached the highest value. By using Rd and CF, the change of notch impact strengths of the PLA/biomass filler composites showed a similar trend with the use of WS. With the introduction of 40% Rd and CF, the notch impact strengths of the PLA/biomass filler composites were  $4.50 \pm 0.73$  and  $5.36 \pm 0.20 \text{ kJ/m}^2$ , respectively, which were 2.06–2.46 times higher than that of pure PLA. Shore hardness of pure PLA and the PLA/biomass filler composites was also shown in Fig. 2b. The hardness (Shore D) of pure PLA was only 86. With the addition of biomass fillers (Rd, WS, and CF) at 40%–60%, the Shore hardness of the composites was improved to  $\sim 90$  after processing.



**Figure 2:** Notch impact strength (a) and hardness (Shore D) (b) of PLA/biomass filler composites with reed, wheat stalk, and coconut fiber

From the data of mechanical properties shown in Figs. 1 and 2, it was understood that the introduction of the biomass fillers (particular Rd) to PLA can contribute good comprehensive performances containing stiffness, flexural strength, and impact toughness to the PLA/biomass filler composites. In comparison with the PLA based composites prepared with other commonly used powdery biomass fillers (for example, starch [23], bamboo powder [20], and microcrystalline cellulose [24]), without additional compatibilizer and reactive toughening agent in the composites, it was rather good that the flexural strength of the obtained PLA/biomass filler composites did not decrease significantly and the impact strength increases a lot under the condition of the amount of biomass filler at 40%–50%. That was because the structure and morphology of biomass filler produce an important impact to the mechanical properties of the composites.

### 3.2 Structure and Morphology of Biomass Filler in Composite

Fig. 3 shows the FT-IR spectra of the raw materials (including PLA and biomass fillers) and PLA/biomass filler composites with reed, wheat stalk and coconut fiber at 30% and 60%. FT-IR tests of the raw materials (including PLA and biomass fillers) and PLA/biomass filler composites with reed, wheat stalk and coconut fiber were shown in Fig. 3a. No adsorption appeared in 3700–3100  $\text{cm}^{-1}$  of pure PLA due to the rareness of terminal O–H groups. Two absorption bands at around 2995 and 2945  $\text{cm}^{-1}$  were shown on the FT-IR curve of PLA. It was attributed to –CH– stretching vibration of PLA. A very strong absorption peak concerning the stretching vibration of –C=O appeared at  $\sim 1751 \text{ cm}^{-1}$ . These were the two most important characteristic peaks of PLA in the composites [25]. Besides, there also showed some other absorption bands at 1182, 1127, 1082 and 1044  $\text{cm}^{-1}$  on the FT-IR curve of the pure PLA. They were known as the vibration of –C–O– groups. As to the biomass fillers of CF, SW and Rd, all of them were mainly composed by cellulose, lignin and hemicellulose. They showed similar adsorption band at  $\sim 3300$ ,  $\sim 2925$ ,  $\sim 2860$  and  $\sim 2350 \text{ cm}^{-1}$ , which were related to the groups of O–H and –CH– on the biomass fillers [26], respectively (see Fig. 3a). After blended PLA with the biomass fillers at 30% and 60%, it exhibited the similar FT-IR curves in Fig. 3b. The absorption bands at 2995 and 1751  $\text{cm}^{-1}$  reflected the component of PLA. The absorption bands at  $\sim 2925$ ,  $\sim 2860$  and  $\sim 2350 \text{ cm}^{-1}$  belong to the component of the biomass fillers. Therefore, the difference between mechanical properties of the various PLA/biomass filler composites should be mainly subject to by the physical structure and morphology of the biomass fillers.

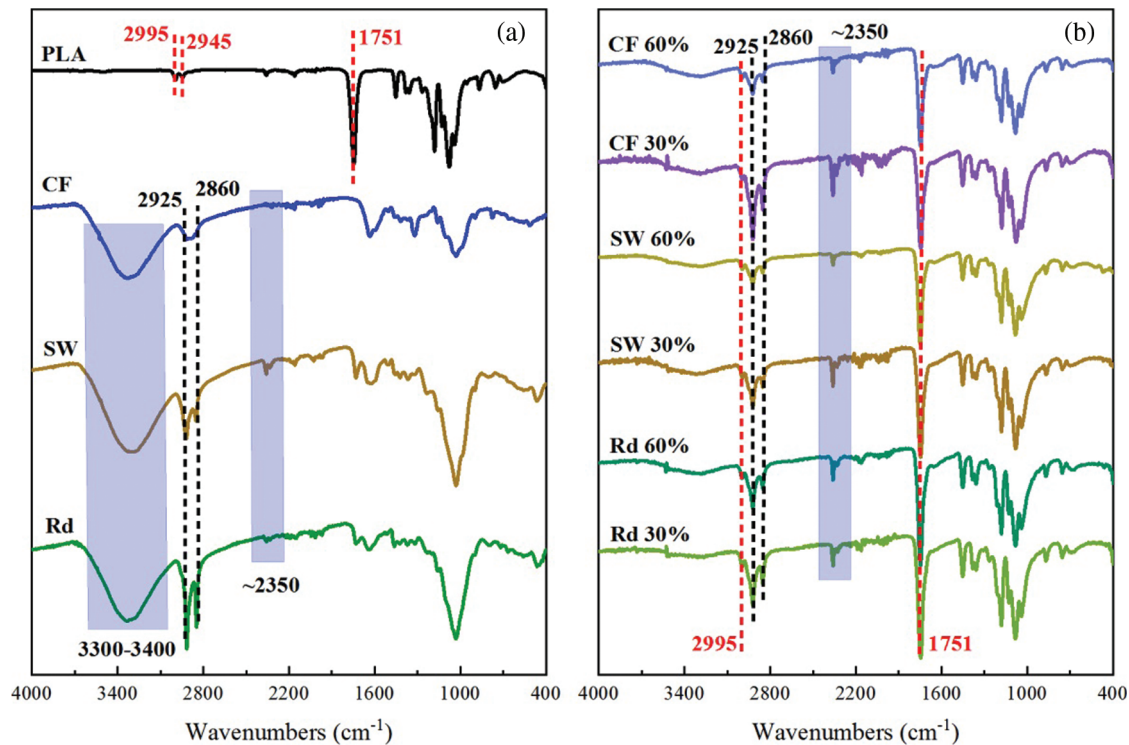


**Figure 3:** FT-IR spectra of raw materials (a) and PLA/biomass filler composites (b) with reed, wheat stalk and coconut fiber

Observation of the section of PLA/biomass filler composites can clearly show the morphology of biomass fillers. From Fig. 4, Rd, WS, and CF showed the size at the scale of several millimeters. The inner part of these biomass filler had the micro-fibrous structure originated from natural plant fiber. Particularly, in the composites with 60% biomass filler, these biomass fillers presented a crisscross arrangement (Figs. 4d–4f). Around the biomass filler, no obvious cavity or hole existed. That was to say, even if the composite was filled with high content of biomass filler, there still had good compatibility between PLA and biomass filler. Before processing, the size of Rd, WS, and CF was up to 1–2 cm (see Figs. 5a–5c). After blending with PLA, Rd and WS still showed relatively thick morphology (Figs. 5a and 5b). The length of Rd was around 0–3.6 mm with the major distribution at ~1.3 mm (Fig. 5d) and the diameter was mainly around 0.6 mm (Fig. 5g). As to WS, the length was distributed at ~1.3 mm (Fig. 5e), which was similar with the situation of Rd. But, the diameter of WS was at 0.8 mm (Fig. 5h), which was a little larger than the diameter of Rd. However, CF exhibited a relatively larger length at the distribution of ~1.8 mm (Fig. 5f). Its diameter was rather low at 0.2–0.3 mm (Fig. 5i).

Along with the understanding of the flexural properties of the PLA/biomass filler composites as shown in Fig. 1, it can be deduced that Rd induced the optimal comprehensive performance. The flexural moduli and flexural strengths of the PLA/biomass filler composites with WS were lower than those of the composites with Rd. As to CF, it produced the highest flexural strength and the lowest flexural modulus of the PLA/biomass filler composites. As to the impact toughness shown in Fig. 2, the PLA/biomass filler composite with WS had the highest impact strength. And the impact strengths of the PLA/biomass filler composites with Rd and CF decreased in turn.

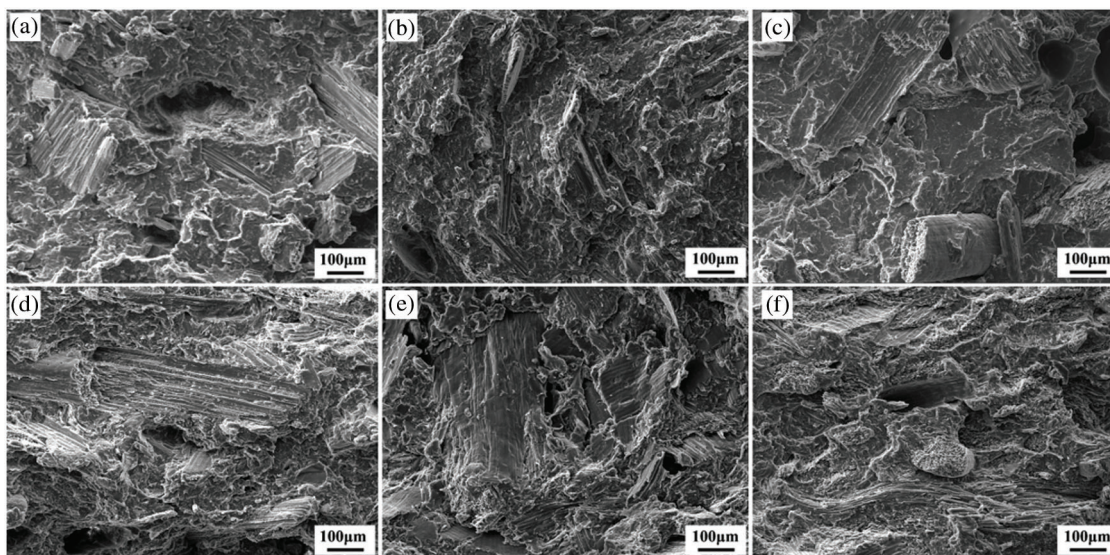


**Figure 4:** SEM micrographs of PLA/biomass filler composites with reed (a, d), wheat stalk (b, e) and coconut fiber (c, f) at 30% (a, b, c) and 60% (d, e, f)

### 3.3 Thermal Properties and Water Absorption

TGA analysis of PLA/biomass filler composites is shown in Fig. 6 and Table 1. Among these composites, the PLA/biomass filler composites with Rd exhibited the highest initial decomposition temperature ( $T_{5\%}$ ) at 289.4°C (30%) and 274.5°C (60%). The residual mass of the PLA/biomass filler composites with 30% and 60% Rd at 800°C ( $M_{800}$ ) was 5.5% and 13.2%, respectively. After blending WS and CF in PLA, the initial decomposition temperature of the PLA/biomass filler composites decreased to 229.9°C–273.7°C. As far as we know, Rd, WF and CF are mainly composed by cellulose, lignin and hemicellulose. Cellulose has the highest thermal decomposition temperature (over 300°C). However, the initial thermal decomposition temperature of lignin is the lowest at 150°C–160°C. Hemicellulose starts to decompose by heat at about 170°C–180°C. And the heating rate reaches the highest at 190°C–210°C. Among the PLA composites with the three biomass fillers, CF had the highest content of lignin (at ~35.9%). It induced the lowest  $T_{5\%}$  of the composites (see Table 1). As to PLA/WF composites, although the amount of lignin was lower than PLA/Rd composites, the content of hemicellulose in the composites was much higher. The  $T_{5\%}$  of PLA/WF composites was lower than that of PLA/Rd composites. In addition, the amount of residual mass at 800°C of the composites with WS and CF was very similar to the PLA/biomass filler composites with Rd. The introduction of biomass filler in PLA composites produced some solid residue in TGA test. From Table 1, there was no residual mass of pure PLA. With 60% biomass fillers (including Rd, WF and CF),  $M_{800}$  was 13%–17%.

DSC analysis of the PLA/biomass filler composites was also carried out. As shown in Fig. 7a, pure PLA had a cold crystallization peak at 96.1°C. After adding biomass fillers, the cold crystallization temperature of the PLA/biomass filler composites (with Rd, WS, and CF) slightly decreased. That was because the addition of biomass filler in PLA composites introduces the crystallization nucleation center of PLA. It improves the crystallization rate of PLA. As a result, the temperature of cold crystallization of PLA decreases. Furthermore, the high amount of biomass filler in composites could induce high crystallization rate of PLA. By increasing the content of biomass filler to 60%, the area of cold crystallization peak obviously decreased. It shows the low temperature of cold crystallization of PLA in comparison with that of the PLA/biomass filler composites with the amount of filler at 30%. To some extent, this phenomenon will cause an increase in the hardness of the composites, as exhibited in Fig. 2b. After adding biomass fillers

(Rd, WS, and CF) in PLA, the PLA/biomass filler composites showed the melting temperature ( $T_m$ ) at around 168°C–176°C (see Table 1). There was no large difference in the melting temperature of pure PLA (174.7°C). Among the three biomass fillers, WS enhanced PLA composites showed the two different melting temperatures. It should be formed by the unstable thermal decomposition of hemicellulose in WS. The pure PLA produced 31.0% crystallinity during processing. After being filled with 30% biomass fillers, the crystallinity of PLA in the composites did not change a lot (Table 1). By the introduction of the amount of biomass fillers to 60%, the crystallinity of the PLA in composites increases to 44.6%–48.8%.

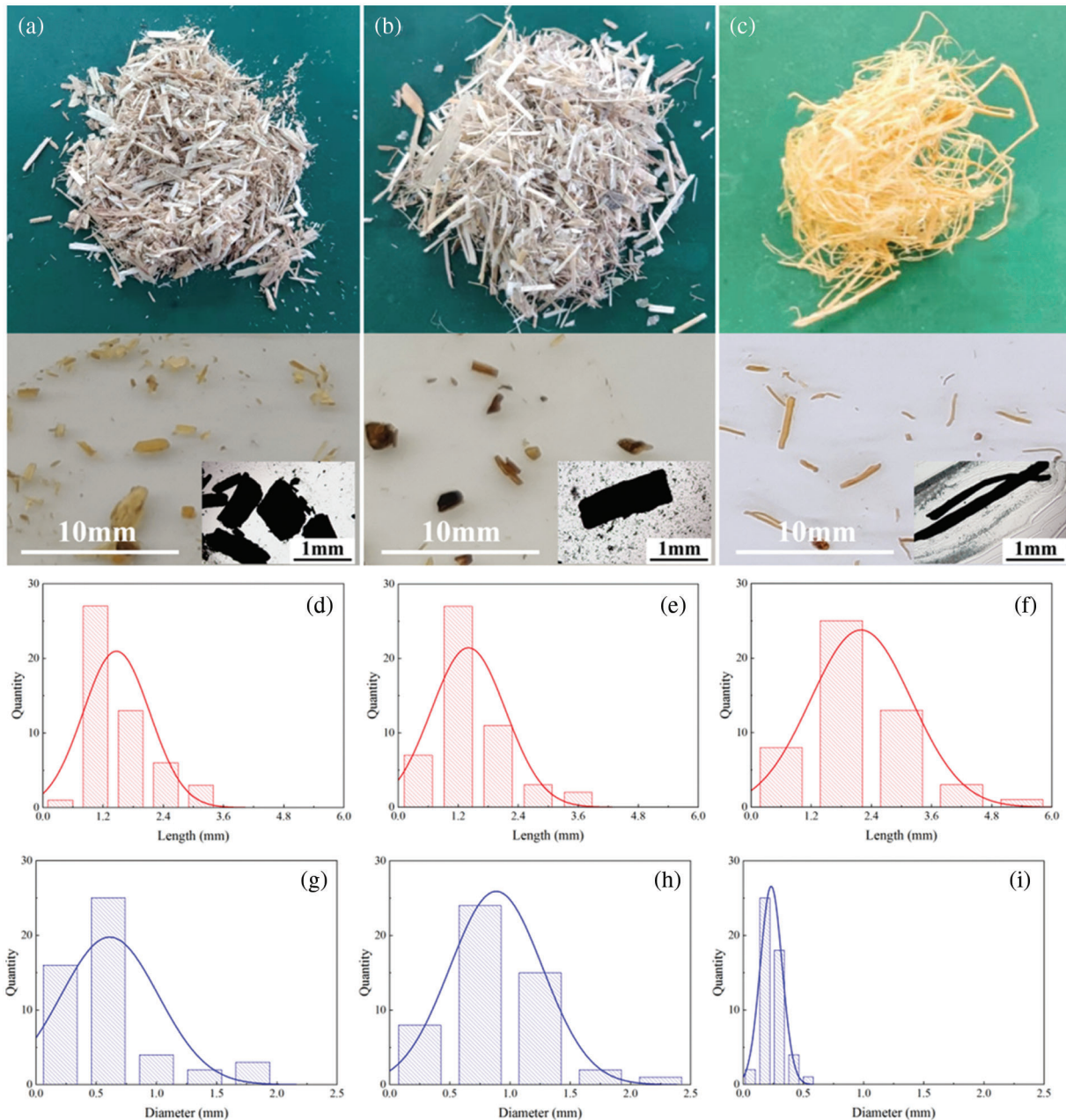


**Figure 5:** Appearance (original and extracted from PLA/biomass filler composites) and size distribution (extraction from PLA/biomass filler composites) of reed (a, d, g), wheat stalk (b, e, h) and coconut fiber (c, f, i)

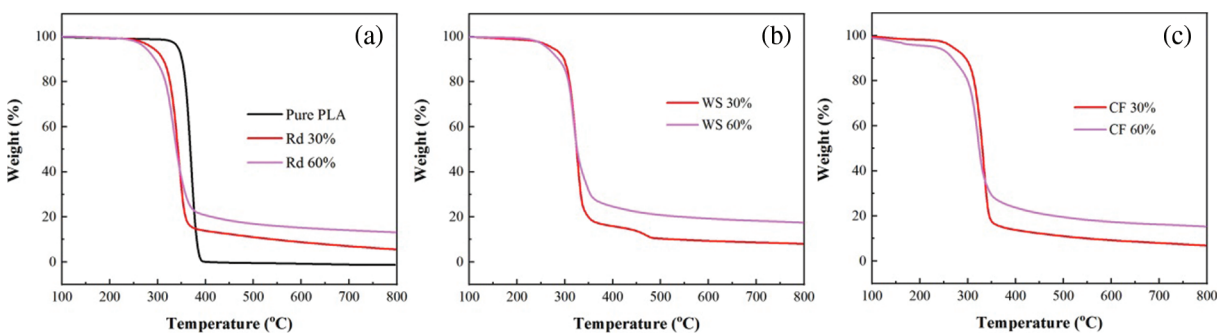


**Figure 6:** TGA analysis of PLA/biomass filler composites with reed (a), wheat stalk (b) and coconut fiber (c)

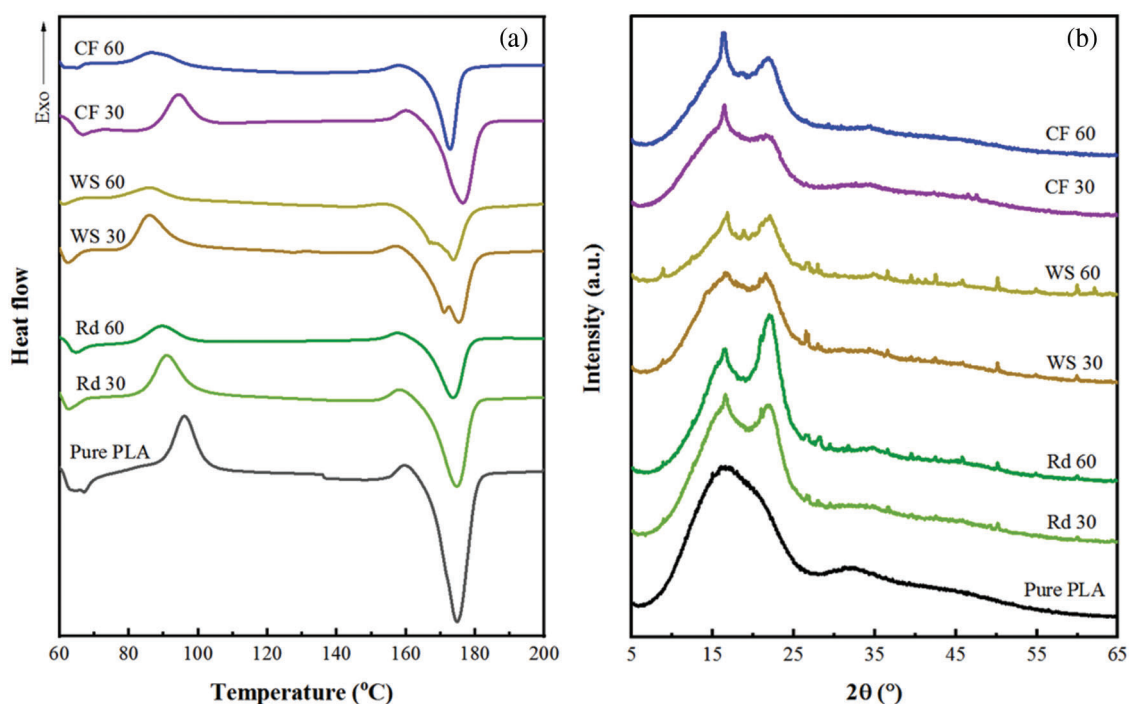


**Figure 7:** DSC thermograms (a) and XRD patterns (b) of PLA/biomass filler composites with reed, wheat stalk and coconut fiber

Fig. 7b gives the XRD patterns of the PLA/biomass filler composites. From the Figure, only a dispersed diffraction peak at  $16.5^\circ$  can be found in the XRD curve of PLA. After adding biomass fillers (including Rd, WS, and CF), it mainly showed a dual peak on the XRD curves. In the experiment, the filled biomass fillers can be used as the nucleation center of PLA. Due to the size of the biomass fillers at the scale of several millimeters, the crystallization of PLA must be along with the surface of biomass fillers. It could produce a certain degree of stretching effect to form the multiple crystal structures of PLA [27], which induced the appearance of dual peaks on the XRD curves.

Table 2 gives the change of mass and size of various PLA/biomass filler composites after soaking in water. After soaking in water with 24 and 48 h, the mass and size of the PLA/biomass filler composites didn't change a lot. It showed rather low water absorption. That was because PLA forms the coating on the surface of biomass fillers during processing. And PLA was a hydrophobic polymer. It will not

produce majority water absorption in a certain period of time. This result is consistent with the current research on polylactic acid and its composites [28].

**Table 2:** The change of mass and size of PLA/biomass filler composites with reed, wheat stalk, and coconut fiber after soaking in water

Samples	Mass (g)			Size (width × thickness) (mm <sup>2</sup> )		
	Original	After 24 h	After 48 h	Original	After 24 h	After 48 h
Pure PLA	3.99	4.00	4.00	10.04 × 4.00	10.03 × 4.00	10.40 × 4.00
Rd 30	4.66	4.70	4.71	10.34 × 4.30	10.35 × 4.35	10.39 × 4.36
Rd 60	4.47	4.61	4.65	10.17 × 4.11	10.32 × 4.13	10.29 × 4.14
WS 30	4.89	4.96	4.97	10.21 × 4.54	10.23 × 4.60	10.28 × 4.62
WS 60	5.11	5.34	5.39	10.21 × 4.46	10.35 × 4.70	10.42 × 4.72
CF 30	4.72	4.78	4.79	10.37 × 4.60	10.40 × 4.66	10.38 × 4.68
CF 60	4.92	5.05	5.09	10.32 × 4.55	10.46 × 4.57	10.42 × 4.60

#### 4 Conclusions

PLA/biomass filler composites containing biomass fillers such as Rd, WS, and CF (namely HPCs) with the length and diameter at the scale of several millimeters were prepared. Without using additional compatibilizer and toughening agent, the PLA/biomass filler composites still exhibited fairly good stiffness, flexural strength, and impact toughness. Results showed the biomass fillers mainly affected the mechanical properties of the PLA/biomass filler composites. Among the three kinds of biomass fillers, reed reinforced PLA composites show optimal mechanical properties. With 40%–50% Rd, the PLA/biomass filler composites showed flexural modulus over 7000 MPa. Flexural strength basically remained at the same level of pure PLA. And the notch impact strength reached  $4.50 \pm 0.73$  kJ/m<sup>2</sup>, which was 2.06 times higher than that of pure PLA. In addition, the introduction of biomass fillers increased the crystallization ability of PLA and did not increase the water absorption of the composites.

**Funding Statement:** This research is supported by “One Belt, One Road” Projects of China Academy of Sciences (174433KYSB20190082), Science and Technology Service Network Plan of China Academy of Sciences (KFJ-ST-S-QYZD-2021-16-002), Key Projects of Ningbo Public Welfare Science and Technology Plan (2021S020), Ningbo Natural Science Foundation (2021J196), and Youth Innovation Promotion Association CAS (2017339).

**Conflicts of Interest:** The authors declare that they have no conflicts of interest to report regarding the present study.

#### References

1. Zhao, B. J., Hu, Y. L., Gao, J. H., Zhao, G. B., Ray, M. B. et al. (2020). Recent advances in hydroliquefaction of biomass for bio-oil production using in situ hydrogen donors. *Industrial & Engineering Chemistry Research*, 59(39), 16987–17007. DOI 10.1021/acs.iecr.0c01649.
2. Tzelepi, V., Zeneli, M., Kourkoumpas, D. S., Karampinis, E., Gypakis, A. et al. (2020). Biomass availability in Europe as an alternative fuel for full conversion of lignite power plants: A critical review. *Energies*, 13(13), 3390. DOI 10.3390/en13133390.

3. Yu, Q., Wang, Y. C., van Le, Q., Yang, H., Hosseinzadeh-Bandbafha, H. et al. (2021). An overview on the conversion of forest biomass into bioenergy. *Frontiers in Energy Research*, 9, 684234. DOI 10.3389/fenrg.2021.684234.
4. Liu, X. F., Yang, W. J., Zhang, Q. Y., Li, C., Wu, H. G. (2020). Current approaches to alkyl levulinates via efficient valorization of biomass derivatives. *Frontiers in Chemistry*, 8, 794. DOI 10.3389/fchem.2020.00794.
5. Sarker, T. R., Nanda, S., Dalai, A. K., Meda, V. (2021). A review of torrefaction technology for upgrading lignocellulosic biomass to solid biofuels. *Bioenergy Research*, 14(2), 645–669. DOI 10.1007/s12155-020-10236-2.
6. Qiao, Y., Feng, L. X., Li, Z. Q., Zhang, Z. Y., Chen, J. et al. (2020). Effect of adsorption of ZrO<sub>2</sub> in catalysts on the efficiency of hydrolysis of cellulose to sugar in aqueous system under microwave radiation. *Chinese Journal of Chemistry*, 38, 399–405.
7. Wang, H. B., Zhang, X. F., Guo, S. Y., Liu, T. (2021). A review of coextruded wood-plastic composites. *Polymer Composites*, 42(9), 4174–4186.
8. Mokhena, T. C., Sadiku, E. R., Mochane, M. J., Ray, S. S. (2021). Mechanical properties of fire retardant wood-plastic composites: A review. *Express Polymer Letters*, 15(8), 744–780.
9. Naumann, A., Seefeldt, H., Stephan, I., Braun, U., Noll, M. (2012). Material resistance of flame retarded wood-plastic composites against fire and fungal decay. *Polymer Degradation and Stability*, 97(7), 1189–1196.
10. Ashori, A. (2008). Wood-plastic composites as promising green-composites for automotive industries! *Bioresource Technology*, 99(11), 4661–4667.
11. Wu, Q. L., Chi, K., Wu, Y. Q., Lee, S. (2014). Mechanical, thermal expansion, and flammability properties of co-extruded wood polymer composites with basalt fiber reinforced shells. *Materials & Design*, 60(4), 334–342. DOI 10.1016/j.matdes.2014.04.010.
12. Matuana, L. M., Jin, S., Stark, N. M. (2011). Ultraviolet weathering of HDPE/wood-flour composites coextruded with a clear HDPE cap layer. *Polymer Degradation and Stability*, 96(1), 97–106. DOI 10.1016/j.polymdegradstab.2010.10.003.
13. Zhou, L., Ke, K., Yang, M. B., Yang, W. (2021). Recent progress on chemical modification of cellulose for high mechanical-performance poly (lactic acid)/Cellulose composite: A review. *Composites Communications*, 23, 100548. DOI 10.1016/j.coco.2020.100548.
14. Jodlowski, G. S., Strzelec, E. (2021). Use of glycerol waste in lactic acid bacteria metabolism for the production of lactic acid: State of the art in Poland. *Open Chemistry*, 19(1), 998–1008. DOI 10.1515/chem-2021-0073.
15. Li, G., Zhao, M. H., Xu, F., Yang, B., Li, X. Y. et al. (2020). Synthesis and biological application of polylactic acid. *Molecules*, 25(21), 5023. DOI 10.3390/molecules25215023.
16. Kian, L. K., Saba, N., Jawaid, M., Sultan, M. T. H. (2019). A review on processing techniques of bast fibers nanocellulose and its polylactic acid (PLA) nanocomposites. *International Journal of Biological Macromolecules*, 121(2), 1314–1328. DOI 10.1016/j.ijbiomac.2018.09.040.
17. Getme, A. S., Patel, B. (2020). A review: Bio-fiber's as reinforcement in composites of polylactic acid (PLA). *Materials Today: Proceedings*, 26(1), 2116–2122. DOI 10.1016/j.matpr.2020.02.457.
18. Zhu, L. X., Qiu, J. H., Liu, W. D., Sakai, E. (2019). Mechanical and thermal properties of rice Straw/PLA modified by nano Attapulgit/PLA interfacial layer. *Composites Communications*, 13(8), 18–21. DOI 10.1016/j.coco.2019.02.001.
19. Sinha, A. K., Bhattacharya, S., Narang, H. K. (2021). Abaca fibre reinforced polymer composites: A review. *Journal of Materials Science*, 56(7), 4569–4587. DOI 10.1007/s10853-020-05572-9.
20. Na, H. N., Huang, J. C., Xu, H. G., Bao, X., Xie, L. K. et al. (2022). Effect of high content filling jute fiber with large aspect ratio on structure and properties of PLA composite. *Polymer Composites*, 43(3), 1429–1437. DOI 10.1002/pc.26463.
21. Fujiura, T., Sakamoto, K., Tanaka, T., Imaida, Y. (2008). A study on preparation and mechanical properties of long jute fiber reinforced polylactic acid by the injection molding process. *4th International Conference on High Performance Structures and Materials*, Algarve, Portugal: Wessex Institute of Technology.

22. Liu, R., Peng, Y., Cao, J. Z., Chen, Y. (2014). Comparison on properties of lignocellulosic flour/polymer composites by using wood, cellulose, and lignin flours as fillers. *Composites Science and Technology*, 103, 1–7. DOI 10.1016/j.compscitech.2014.08.005.
23. Xiong, Z., Dai, X. Y., Zhang, R. Y., Tang, Z. B., Na, H. N. et al. (2014). Preparation of biobased monofunctional compatibilizer from cardanol to fabricate polylactide/starch blends with superior tensile properties. *Industrial & Engineering Chemistry Research*, 53(26), 10653–10659. DOI 10.1021/ie500844m.
24. Dai, X. Y., Xiong, Z., Ma, S. Q., Li, C., Wang, J. G. et al. (2015). Fabricating highly reactive bio-based compatibilizers of epoxidized citric acid to improve the flexural properties of polylactide/microcrystalline cellulose blends. *Industrial & Engineering Chemistry Research*, 54(15), 3806–3812. DOI 10.1021/ie504904c.
25. Ma, X. F., Yu, J. G., Wang, N. (2006). Compatibility characterization of poly(lactic acid)/poly(propylene carbonate) blends. *Journal of Polymer Science*, 44, 94–101.
26. Prosper, N. K., Zhang, S. Y., Wu, H. P., Yang, S. X., Li, S. J. et al. (2018). Enzymatic biocatalysis of bamboo chemical constituents to impart antimold properties. *Wood Science and Technology*, 52(3), 619–635. DOI 10.1007/s00226-018-0987-0.
27. Kangwanwatthanasiri, P., Suppakarn, N., Ruksakulpiwat, C., Ruksakulpiwat, Y. (2015). Glycidyl methacrylate grafted polylactic acid: Morphological properties and crystallization behavior. *Macromolecular Symposia*, 354(1), 237–243. DOI 10.1002/masy.201400094.
28. Tham, W. L., Poh, B. T., Ishak, Z. A. M., Chow, W. S. (2016). Characterisation of water absorption of biodegradable poly(lactic acid)/halloysite nanotube nanocomposites at different temperature. *Journal of Engineering Science*, 12, 13–25.